Relating spatial distributions of acoustically determined patches of fish and plankton: data viewing, image analysis, and spatial proximity

Gordon Swartzman, Richard Brodeur, Jeffrey Napp, Danny Walsh, Roger Hewitt, David Demer, George Hunt, and Elizabeth Logerwell

Abstract: We developed a point-and-click acoustic data viewer (FishViewer) for exploratory comparison of up to three acoustic survey transects (or three frequencies) at a time and other environmental and biological data (e.g., surface temperature and seabird abundance). FishViewer also contains image-processing tools (e.g., morphological and threshold filters) for distinguishing between fish shoals and plankton patches and for patch identification. These tools and methods are illustrated using survey data collected at three frequencies (38, 120, and 200 kHz) near the Pribilof Islands, Bering Sea, during September 1995. Data were also visualized by converting the patches identified in the acoustic images to polygons, showing the boundaries of each patch using a connected component algorithm. Proximity between these fish shoal and plankton patch polygons was examined statistically using an interval-based nonparametric regression model (generalized additive models) and a distance-based proximity measure. The methods presented for data refinement, visualization, and the establishment of fish–plankton patch proximity serve as a paradigm for scale-robust hypothesis formulation and testing of spatial patterns of fish and plankton.

Résumé : Nous avons mis au point un visualiseur de données acoustiques à pointage-cliquage (FishViewer) permettant la comparaison exploratoire de trois transects de détection acoustique (ou de trois fréquences) à la fois, et d'autres données environnementales ou biologiques (p.ex. la température de surface et l'abondance des oiseaux de mer). Le FishViewer comporte aussi des outils de traitement des images (p.ex. un filtre morphologique et un filtre de seuillage) permettant de différencier les bancs de poissons et les essaims de plancton, et de les identifier. Nous illustrons ces outils et méthodes à l'aide de données acoustiques recueillies à trois fréquences (38, 129 et 200 kHz) près des îles Pribilof, en mer de Béring, en septembre 1995. Nous avons aussi visualisé les données en convertissant en polygones les taches identifiées sur les images acoustiques, et en représentant les limites de chaque tache à l'aide d'un algorithme des composantes reliées. La proximité entre ces polygones des bancs de poissons et des essaims de plancton a été examinée statistiquement à l'aide d'un modèle de régression non paramétrique à intervalles (modèles additifs généralisés) et une mesure de proximité basée sur la distance. Les méthodes présentées pour raffiner et visualiser les données et établir la proximité des bancs de poissons et des essaims de plancton servent de paradigme pour la formulation d'hypothèses robustes quelle que soit l'échelle et pour la mise à l'essai des régimes spatiaux des poissons et du plancton.

[Traduit par la Rédaction]

Introduction

Pelagic fish and plankton spatial distributions in ocean ecosystems are influenced by hydrologic features such as ocean fronts and eddies, thermal stratification, and upwelling (Mann and Lazier 1991; Mullin 1993). As a result of the interaction between animal behavior and these physical processes, large patches of zooplankton develop and are maintained. These patches may attract planktivorous fish (Mackas et al. 1985, 1997; Barange 1994). These in turn serve as attractors to piscivorous fish, seabirds, and marine mammals. The large spatial scale in oceanic systems and the lack of consistent methods for acoustically distinguishing fish shoals from plankton patches have allowed only limited study of the spatial interrelationship of fish and zooplankton in the open ocean.

In this paper, we introduce methods for describing the spatial interrelationship of fish shoals and plankton patches. Our objectives are to (*i*) describe a point-and-click acoustic data viewer (FishViewer) and its utility for visualizing and

Received October 20, 1997. Accepted September 8, 1998.
J14264

G. Swartzman.[1] Applied Physics Laboratory, 355640 University of Washington, Seattle, WA 98195, U.S.A.
R. Brodeur and J. Napp. Alaska Fisheries Science Center, NMFS, Seattle, WA 98115, U.S.A.
D. Walsh. Statistics Department, University of Washington, Seattle, WA 98195, U.S.A.
R. Hewitt, D. Demer, and E. Logerwell. Southwest Fisheries Science Center, NMFS, La Jolla, CA 92038-0271, U.S.A.
G. Hunt. Department of Ecology and Evolutionary Biology, University of California, Irvine, CA 92697, U.S.A.

[1]Author to whom all correspondence should be addressed. e-mail: gordie@alava.apl.washington.edu

Fig. 1. Pribilof Island study region in the eastern Bering Sea showing the locations of the A, B, C, and D transect lines.

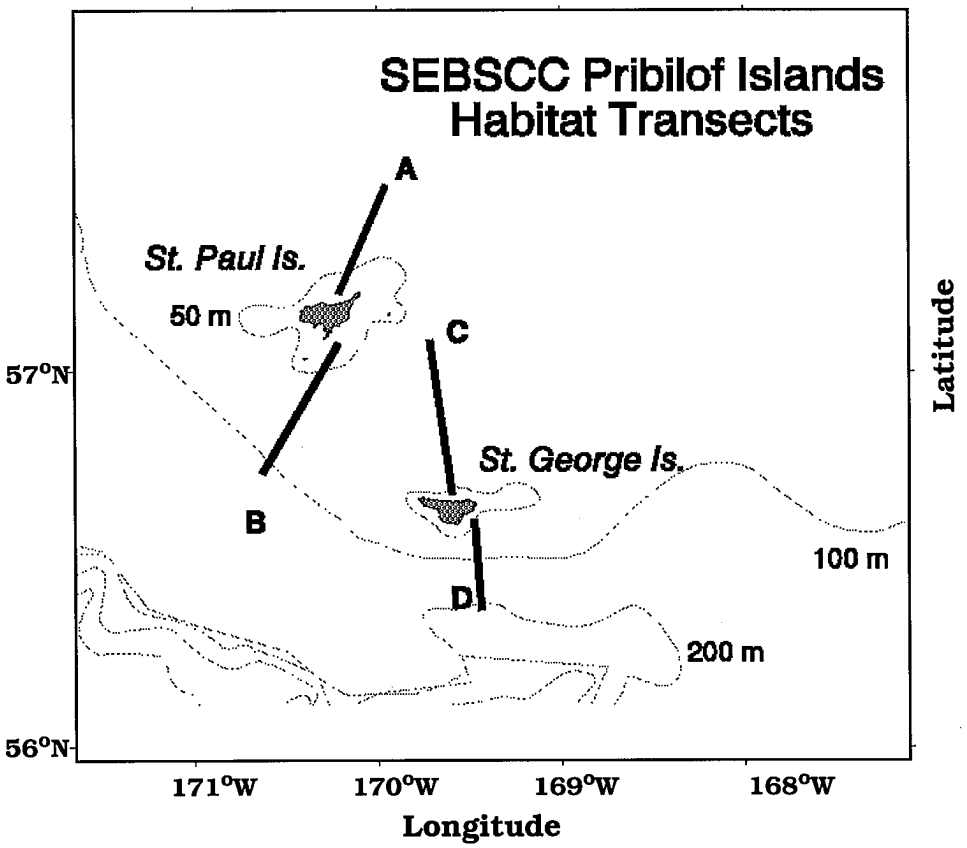

exploring multivariable spatial data sets, (*ii*) introduce recent developments in proximity analysis for describing the spatial interrelationships between predators and prey, and (*iii*) compare two proximity methods and insights into juvenile walleye pollock (*Theragra chalcogramma*) and zooplankton spatial relationships in the eastern Bering Sea (Fig. 1) during September 1995 (Brodeur et al. 1997).

Because of the large amount of data collected by acoustic surveys and the intensive computational nature of the image-processing methods used to identify plankton and fish aggregations, we have developed a viewer to display the different types of data and aid experimentation with the analysis methods used. This viewer has allowed us to develop and evaluate aggregation detection methods as well as to provide a visual exploratory analysis tool.

A major challenge of our work has been to develop and test methods to establish the degree of proximity among plankton, juvenile fish, and seabirds. We desired a proximity measure that considers the patchy nature of both fish and plankton as well as other factors such as the diel migration of plankton and the diel feeding pattern of the birds. In the study area the patches are large enough that they "fill" a significant portion of the surveyed transects; therefore, they cannot be treated as points in space, as is common with spatial statistical measures of interpatch distance. Proximity is complicated by the differential diel movements of plankton and fish such that the patches may be vertically separated at certain times of the day, even though they are horizontally close in space. A proximity measure that addresses how predators orient relative to prey patches should include features of patch size, orientation, and edge-to-edge, rather than center-to-center, distance. Also, the measure of proximity should include a randomness null hypothesis (i.e., the plankton and fish patches are randomly distributed in space relative to each other) and a method for testing the empirical distribution against the null hypothesis.

Methods

Exploratory viewing of acoustic and environmental data

Exploratory analysis of the acoustic data and supporting environmental and biological data collected along the study transects was made possible through the development of FishViewer (Fig. 2), a point-and-click display tool. FishViewer was developed following a prototype system (Lascara 1997) used to display oceanographic data from a towed recorder system. FishViewer adds many features specific to acoustic data and their analysis. It is written in the PV-WAVE echogram-processing programming language and allows the following operations: (*i*) loads transect acoustic echograms into any of three display panels, (*ii*) overlays seabird, surface temperature, salinity, or fluorescence or CTD isotherms along the transect filters on any echogram, (*iii*) performs morphological filtering with a choice of structuring elements and operations, (*iv*) performs pixel-by-pixel differencing between any two compatible echograms, (*v*) allows changing color tables for the acoustic displays, (*vi*) allows examination of the entire acoustic transect using slider bars, and (*vii*) samples backscatter at a point or along a line and displays backscatter values or histograms.

Fig. 2. FishViewer point-and-click acoustic echogram viewer showing data from 1995 transect A at three frequencies. Data were collected from two vessels in close proximity. Bird locations and isotherms can be overlaid on any of the acoustic echogram panels.

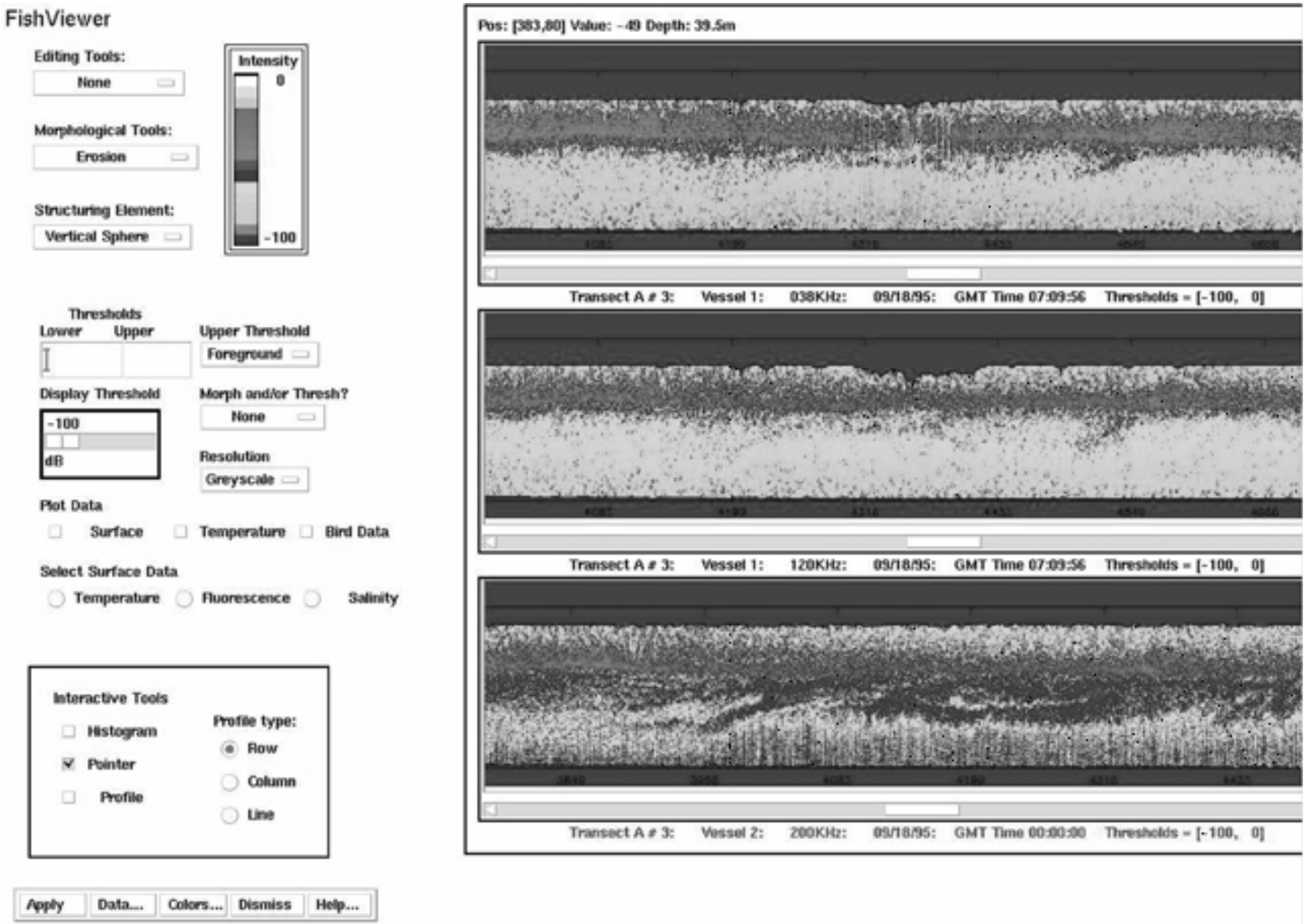

Acoustic surveys

Data for the demonstration of FishViewer and spatial analysis of fish and zooplankton are from acoustic surveys near the Pribilof Islands (Brodeur et al. 1997). Briefly, National Oceanographic and Atmospheric Administration research vessels *Miller Freeman* and *Surveyor* sampled hydrography, nekton, plankton, and seabird distributions in tandem along a 50-km transect extending north from St. Paul Island, Alaska (transect A, Fig. 1), during September 1995. Nominal separation of the two ships was 0.4 km, and speed ranged from 8 to 16 $km \cdot h^{-1}$. Echo integration and target strength measurements (Simrad EK-500 split-beam echosounder and BI-500 analysis software) were collected for three frequencies (38 and 120 kHz on the *Miller Freeman* and 120 and 200 kHz on the *Surveyor*). Prior to the survey, system gains were calibrated using the standard sphere method (Foote et al. 1987). For each transect, measurements of volume backscatter strength (S_v, decibels per cubic metre, 1 μPa at 1 m) at each frequency were recorded each second. The acoustic data were subsampled to produce acoustic echograms with a horizontal resolution of 1000 pixels per 8 km (about 8 m per pixel) and a depth resolution of 0.5 m.

Shoal and patch identification

Fish shoal identification methods used 38-kHz data (Swartzman et al. 1994*a*), while the plankton patch identification used 120- and 200-kHz data. The algorithms required that patches comprise contiguous pixels, with a clearly defined boundary, in a backscatter range indicative of the target species or group (e.g., greater than –54 dB for walleye pollock and between –72 and –55 dB for zooplankton). The backscatter range was chosen with a threshold filter (all pixels outside the expected backscatter range were set to the background level). Morphological filters were then used to highlight patches in the resulting images. Morphological filters are image-processing methods used to separate clearly bounded objects from background noise (Haralick and Shapiro 1992). They apply dilation and erosion operations, using a predefined structuring element, to an image. Filters can be either binary (0–1) or grayscale. The dilation operation can be visualized as increasing the value of pixels surrounded by pixels at a higher level, up to the level of the surrounding pixels, while erosion lowers the value of pixels surrounded by pixels at a lower level to that level. This morphological filter fills small holes, emphasizes the boundary of the patches, breaks small isthmuses between patches, and eliminates small patches (smaller than the structuring element). The influence of surrounding pixels depends on the size (and shape) of the structuring element chosen. By applying dilation and erosion operations in sequences called openings and closings, the morphological filters can clearly define and distinguish bounded objects consisting of contiguous pixels (i.e., patches) from background noise without smearing or smoothing the shape of the object.

Prior to threshold and morphology filtering, the pixels below the bottom and within the bubble layer (about 5 m below the hull mounted echosounders) were removed from the echograms. All operations were programmed in the PV-WAVE higher level, matrix-oriented programming language (Precision Visuals 1992).

For fish shoals, we used a target threshold of pixels above –54 dB in the 38-kHz echogram, based on previous studies of juvenile walleye pollock target strength (Brodeur and Wilson 1996; Traynor 1996). We used a three-pixel horizontal and two-pixel vertical (3 × 2) grayscale structuring element as our morphological filter with a closing and opening operation (Haralick and Shapiro 1992). We then multiplied a binary version of the resultant echogram (0 for background and 1 for included pixels) by the original 38-kHz echogram. The resulting echogram had backscatter levels from the original echogram for all the pixels in identified patches and background backscatter levels (–100 dB) for all pixels not in patches.

To identify zooplankton patches comprising the acoustic backscatter, we took the difference in mean S_v at two frequencies ($S_{v200} - S_{v120}$). If the dominant scatterers contained gas bladders (e.g., juvenile fish) or were large relative to both wavelengths (backscattering cross section >0.75 and 1.25 cm, respectively), then the S_v differences were expected to be negative (due to the resonant effects) or slightly positive (due to geometric scattering). If, on the other hand, animals were smaller than both wavelengths (e.g., copepods and euphausiids), then Rayleigh scattering would be observed and we would expect a positive difference ($S_{v200} - S_{v120} > 0$, Clay and Medwin 1977). We first used a background threshold range of –72 to –54 dB for plankton (everything outside the range was set to the background value) in the 200- and 120-kHz echograms. We then performed a pixel-by-pixel differencing in backscatter between the echograms (200 – 120 kHz) and used morphological filters on the resultant binary echogram with pixels having positive differences greater than or equal to 2 dB (to eliminate pixels with small positive differences due to geometric scattering). We applied an opening and a closing with a 3 × 2 pixel binary structuring element, and the resulting echogram was multiplied by the original 200-kHz echogram. This method assumes that organisms such as euphausiids and copepods produce higher backscatter at 200 kHz than at 120 kHz, as indicated by various theoretical models of acoustic backscatter from fluid spheres and bent cylinders (Greenlaw 1979; Holliday and Pieper 1980; Stanton et al. 1993).

An example of FishViewer, using the above acoustic data and shoal and patch identification algorithms, is displayed in Fig. 2. Echograms of the same nighttime transect at three frequencies highlight that (*i*) the strongest backscatter of fish (red pixels) occurs at 38 kHz and (*ii*) plankton patches are not visible at 38 kHz and are most apparent at 200 kHz (blue pixels). The fish are seen as a layer between 20 and 30 m depth, while the plankton appear as a more amorphous patch below and moving into the fish layer. A depth scale (0–60 m), on the left side of the image, is not visible on the part of the display panels shown in Fig. 2, which are lined up to display a feature in the front region of transect A.

FishViewer was used not only to compare acoustic transects at different frequencies, times of day, years, and regions (i.e., different transects), but also to experiment with different morphological operations as a tool in developing and communicating the shoal and plankton patch identification algorithms. Figure 3 shows, in the top two panels, part of a daytime pass of transect A on September 11, 1995, at 120 and 200 kHz. On both panels, background thresholds between –72 and –54 dB were applied, a range suggestive of plankton S_v at these frequencies. All pixels outside this range were set to the background level (–100 dB) and appear as background (black) on the echograms. The bottom panel shows the result of differencing the 200- and 120-kHz echograms (after thresholds), using the same color table as used for the other echograms and then applying closing and opening morphological filters consecutively to the echogram after thresholding at +2 dB. The algorithm located a large patch near the bottom (polygonal boundary highlighted in green in Fig. 2) and a narrow patch near the top of the image (e.g., around 10 m depth).

Establishing plankton–fish proximity

Acoustic data abstraction

While FishViewer provides an effective means for data exploration, the size of the echogram files (about 1 megabyte apiece) makes statistical and quantitative comparative analysis computationally prohibitive, especially for most fisheries acoustic surveys. Our approach has been to extract the patch information from the echograms in the form of descriptive patch tables. A connected component algorithm (Haralick and Shapiro 1992) was used to locate each identified patch, and various descriptive parameters were

Fig. 3. Display panels from FishViewer illustrating the application of the plankton identification algorithm. The top two panels show 120- and 200-kHz acoustic backscatter images for a daytime pass of transect A with a threshold between –54 and –72 dB. The bottom image shows the difference between the 120- and 200-kHz images with a threshold filter at +2 dB and a morphological closing and opening with a 3 × 2 pixel structuring element. The pixels remaining after these operations are assumed to be plankton patches. The convex hull boundary of the large patch in the bottom image is shown in green.

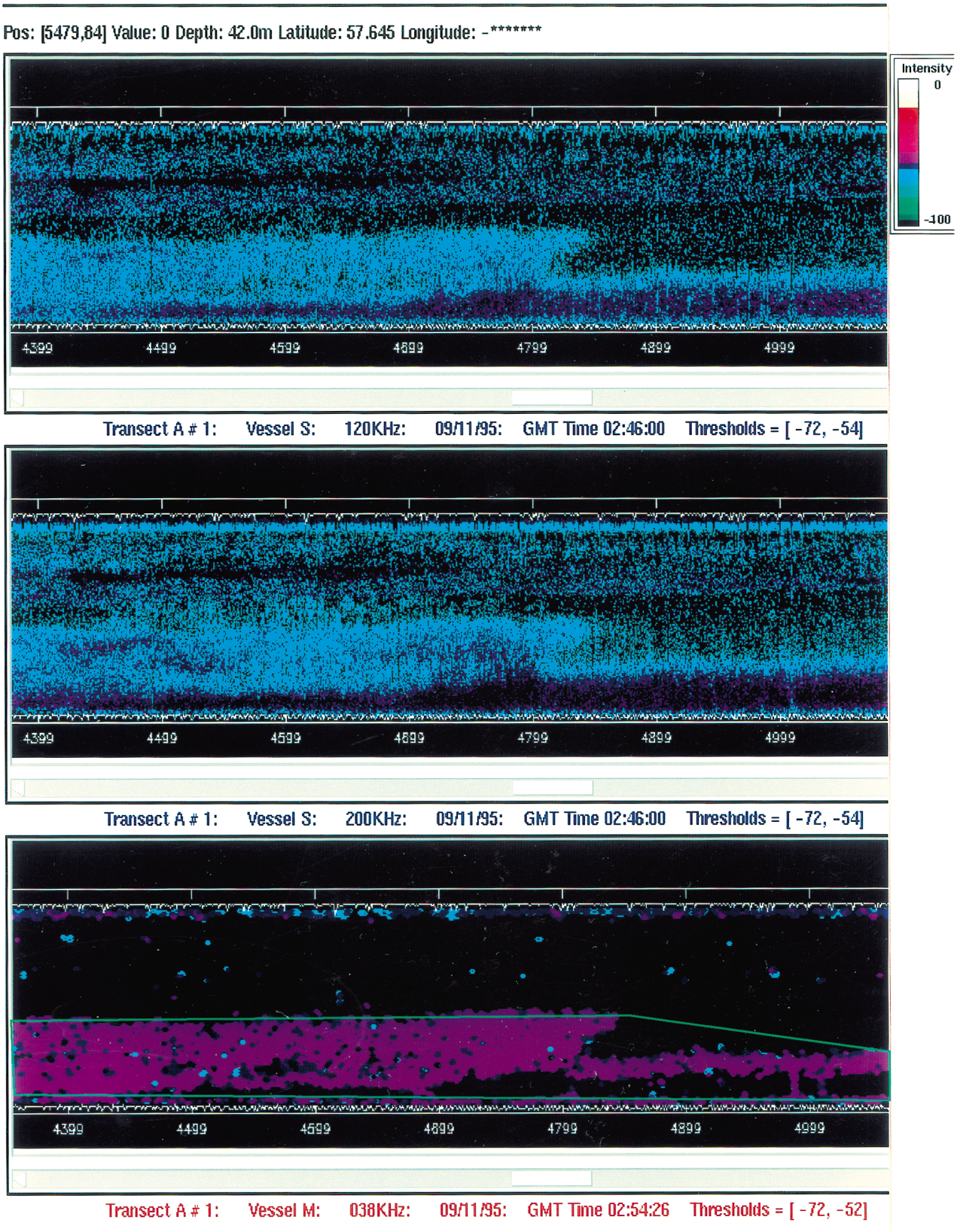

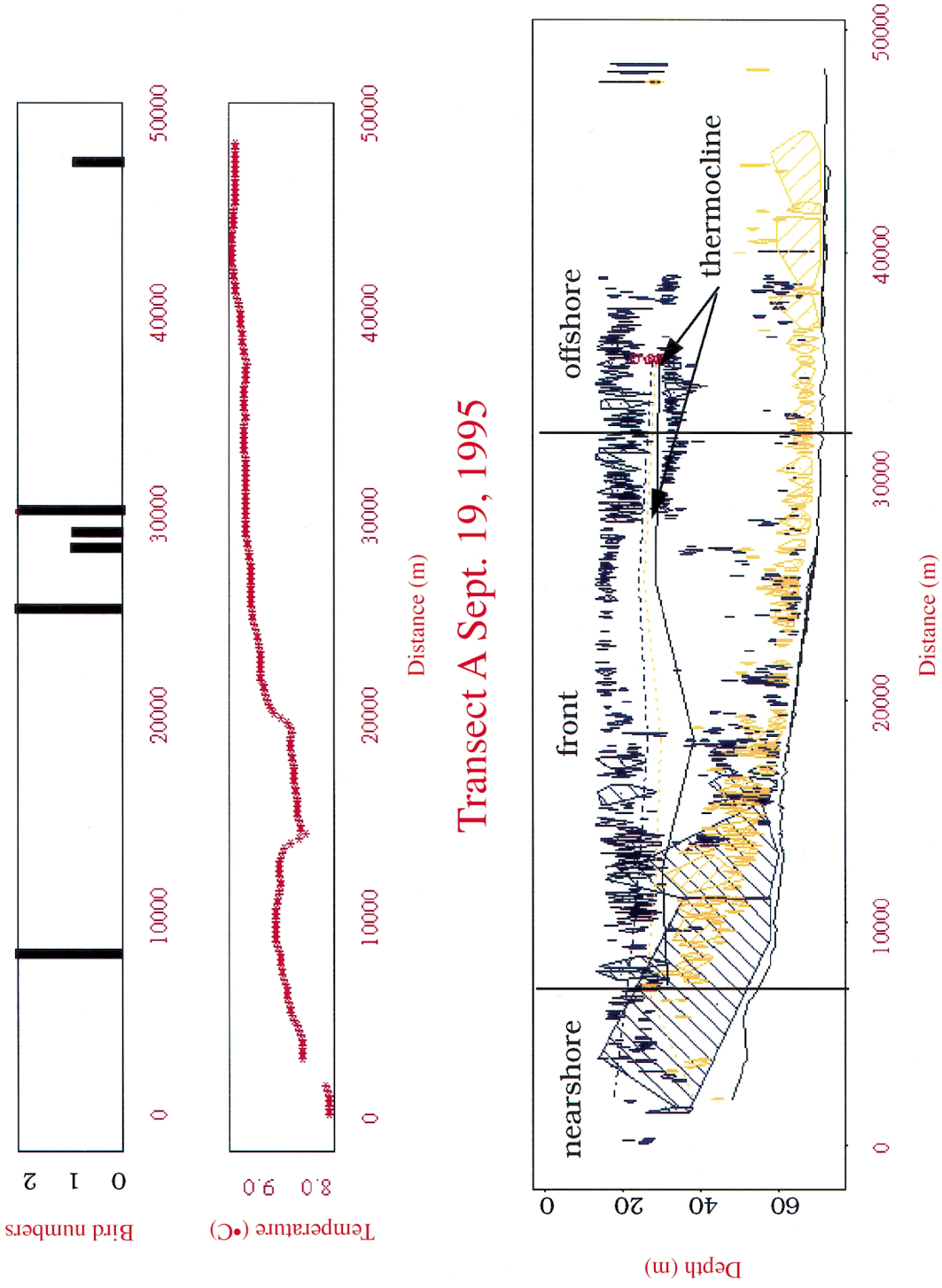

Fig. 4. Polygons showing the shape and location of fish shoals (blue) and plankton patches (orange) in the lower panel, with isotherms along transect A. Surface temperature (middle panel) and the locations of bird sightings (top panel) are also shown. There are no patches visible above 14 m because of the transducer depth. Murre numbers are shown in the top panel.

extracted (Nero and Magnuson 1989) including location parameters (patch depth, latitude, longitude, and distance of the patch center from the start of the transect), size and shape parameters (patch area, width, length, vertices of an eight-sided polygon convex hull enclosing the patch, elongation, and fractal dimension), backscatter parameters (average, maximum, minimum, and variance in patch backscatter), and environmental parameters (depth of the water column below the patch). This table provided a concise description of each patch that was used for display and further analysis of the spatial proximity of plankton and fish patches. Tabular information was entered into the Splus statistical programming language (Becker et al. 1988) for further analyses (described below). Figure 4 shows an example of a daytime pass of transect A on September 19, 1995, with polygons representing the locations of fish shoals and plankton patches (an example of such a polygon is shown in Fig. 3), isotherms calculated from CTD data, and the bottom contour overlaid on the panel. Panels above show surface temperature and the location of birds observed within 300 m of the transect line. This gives a synoptic view of the biota and environmental conditions below and above (i.e., birds) the surface over a 50-km transect.

Binning and generalized additive models

The most straightforward approach to examining spatial proximity between biota is to separate the identified shoals and patches

into horizontal bins or intervals, summing biomass index[2] for all the patches within each bin (Rose and Leggett 1990). Most commonly, within-bin correlations between predator and prey biomass index have been used as a measure of spatial proximity through spectral analysis (Rose and Leggett 1990; Horne and Schneider 1994) or simple correlation calculation (Brown and Morgan 1995). However, these methods are useful only if the relationship between the biota is monotonic. Unspecified nonlinear and nonmonotonic relationships between fish shoals and plankton patches can be included using a nonparametric regression technique, generalized additive models (GAM) (Hastie and Tibshirani 1990). GAM has been used effectively to establish relationships between adult walleye pollock spatial distribution and environmental conditions in the Bering Sea (Swartzman et al. 1994*b*) and between shoals of Pacific hake and environmental conditions in the Eastern Pacific Boundary Current (Swartzman 1997) and herring in the North Sea (Maravelias and Reid 1997). Besides generalizing the assumptions of linearity commonly made in regression and monotonicity made in correlation, GAM also allows a general assumption about the underlying probability distribution, allowing any distribution from the exponential family, which includes the normal, Poisson, binomial, and gamma distributions.

Before using GAM, the data were first binned into horizontal 250-m intervals. A range of intervals from 100 m to 1 km were also used, but the overall results did not change over the range of interval lengths considered. Since many patches spanned several intervals, the fish shoal and plankton patch biomass index was distributed uniformly among all bins that they spanned (assuming that the biomass index was horizontally uniformly distributed within the patch). The data were assumed to have an underlying gamma distribution. The GAM used was

$$\text{Abundance}_{\text{walleye pollock}} = \mu + s(\text{abundance}_{\text{plankton}})$$

where μ is the overall mean and the $s(x)$ are unspecified smooths of the effect of covariate x on the dependent variable. The smoothing in GAM was done using spline smoothers. Visual inspection of the data (e.g., Fig. 4) suggested that the relationship of walleye pollock to plankton was likely to be different in different hydrographic regions. As such, the GAM analysis was done separately for each hydrographic region: a nearshore, tidally mixed region, an offshore, stratified region, and a partially stratified front or transition region. The boundaries between the regions were determined from CTD data using a thermocline-based algorithm that separated the stratified region offshore from the front region and the front from the nearshore region (Stabeno et al. 1999).

Distance-based proximity

An alternative measure of proximity is based explicitly on the distance between patches. Because the plankton diel migrate, it might be misleading to establish that fish and plankton are in the same horizontal bin when they are in fact above and below the thermocline, respectively, although in this case the plankton diel migrate and may be seen as proximate to fish if they are in the same horizontal bin. Alternatively, a fish shoal may be quite far from the center of a plankton patch but quite close to its edge, even when they are not in the same bin. With mobile predators like walleye pollock, we could argue that maintaining proximity does not require being right on top of a prey patch but only within searching distance of the patch. Because of the size of the patches (some plankton patches are over 10 km in horizontal extent), a fish shoal could be some distance from the center of a plankton patch and still have a good chance of encountering it during a feeding period.

Because of the large spatial extent of many plankton patches and fish shoals, a measure of distance between them should not simply be the center-to-center distance, commonly used in spatial statistics as a distance measure between points. Similarly, the measure of proximity of a fish shoal to plankton patches should not simply be the number of plankton patches at different distances from the shoal (however distance is computed) because this ignores the size of or biomass index in the patches. Finally, in order to ascertain whether the observed proximity between fish shoals and plankton patches is "random" or whether prey are clustered around or dispersed away from fish shoals (or vice versa), some measure of randomness is needed.

Our proximity index was based on Ripley's K (Diggle 1983; Cressie 1993), which calculates the number of points inside a circle of radius h from each point in the sample for a range of values of h. Error bounds for randomness are provided by Monte Carlo distribution of the points at random 100 times and repeating the computation of K after each random distribution. Whenever the empirical K goes outside the error bounds, it indicates nonrandomness and shows either clustering (empirical distribution above the error bounds) or inhibition (empirical distribution below the error bounds) in the underlying spatial proximity.

For our study, we replaced the center-to-center distance with an algorithm for computing distance from the edge of a patch to reflect the fact that contact between patches is a function of their edge-to-edge rather than center-to-center distance. We constructed a polygon at distance h from the edge of a patch (analogous to radius h used in Ripley's K) to represent the region at distance h from that patch. Three alternative measures of distance from a patch were considered as follows. (*i*) Construct a polygon h metres both horizontally and vertically away from each patch-edge-polygon vertex. This method allows the mostly horizontally attenuated polygons (Fig. 4) to expand both horizontally and vertically. (*ii*) Construct a polygon h metres out from each patch-edge-polygon vertex along a line from the center of the patch. This method allows proportional growth of the polygon. (*iii*) Ignore vertical distance and take a distance h only in the horizontal direction. This method overcomes the difficulty that gradients in the horizontal and vertical direction are differently perceived by fish and plankton by ignoring the vertical direction entirely.

To identify patches within a distance h from the base polygon, we included those patches having edge vertices (i.e., wholly or partially contained) within the expanded polygon h meters from the original. Instead of counting the number of such patches, we either summed the biomass index for all such patches (or parts of patches) within the expanded polygon or summed the overlap of the patches (or parts of patches) with the original polygon (not the expanded polygon). The overlap measure used was

$$\text{Overlap} = \frac{\text{patch area} + \text{shoal area}}{2(\text{convex hull area})}$$

where the convex hull is a polygon that entirely encloses all boundary points of both original polygons in such a way that a line connecting any two points in either of the enclosed polygons is entirely inside the convex hull polygon. The patch area is the area in square metres of the plankton patch and the shoal area is that of the fish shoal. The overlap measure for any two patches takes a value between 0 and 1. A value of 1 occurs when two patch polygons have 100% overlap, while the value approaches 0 as the patches get farther apart, are more perpendicular to each other in orientation, or are smaller. Figure 5 is a construction of two patches and their convex hull for two contrasting cases. It shows how the overlap changes as edge-to-edge patch distances change.

[2] Biomass index is used as a measure of patch biomass. It is equal to the patch area times the average S_v for the patch and has not been standardized to true biomass, although it is proportional to patch biomass.

Fig. 5. Example of the convex hull (dotted region plus striped regions) for two patches (*a*) partially overlapping and (*b*) farther apart. The overlap measure is close to 1.0 for the patches in Fig. 5*a* and less than 0.5 for those in Fig. 5*b*.

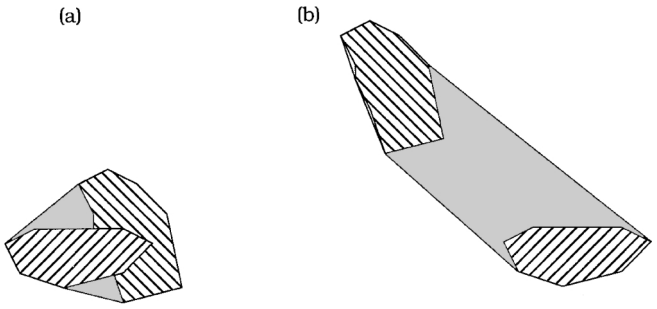

We estimated error bounds for testing the distance-based proximity measure for randomness using a Monte Carlo method. Keeping the original fish shoal locations, plankton patches were uniformly distributed over the region of interest[3] 100 times. The overlap measure was computed for each of these 100 randomizations by growing each fish shoal polygon by distance *h* between 100 m and 1 km and computing the average overlap with patches, over all shoals, as a function of *h*. Random distribution of the patches involved changing the horizontal center of each patch without changing its depth or its shape. This specified "random" to mean a set of patches having the same shape and size as the original patches but being randomly distributed horizontally. As such, it does not address questions about whether the patches have random sizes or are at random depths. We decided to accept depth conditions, as influenced by diel migration, and the existing size distribution of the patches as givens rather than testable factors in the proximity context (i.e., we do not consider what the effect would be if the plankton were not near the bottom during the daytime or what the effect of having a different size distribution of plankton would be on proximity).

The distance-based proximity measure was used to examine the spatial relationship of walleye pollock shoals to plankton patches for the same transect data. Each walleye pollock shoal was "grown" in increments of 100 m from 0 to 1 km as a measure of distance from the shoal. The horizontal measure of distance was used. Thus, we emphasized spatial interrelationships over the same spatial scale used in the GAM study (although only the 250-m interval results were shown). Larger scale overlap (i.e., larger than 1 km) could be investigated, but given the limited size of the transect in each region (e.g., 20 km for the front region), larger scale (i.e., 5–10 km) relationships might not be observable because there would be too few intervals in each region.

Results

Figure 4 shows polygons representing (in iconified form) the size and daytime orientation of fish and plankton patches for a single pass of transect A. Surface temperature and bird abundance are shown by panels on top of the main display, while temperature isotherms are overlaid on the main panel. The transect has a well-mixed nearshore region (no stratification), a front region with partial stratification, and a well-stratified offshore region with a well-defined and narrow thermocline. The distribution of fish and plankton for this day differed among these three regions. The nearshore region (to about 6000 m from the start of the transect) contained small shoals and few plankton. The front region (6000 – 32 000 m) contained many smaller fish shoals above the thermocline with small plankton patches below the thermocline and two large fish shoals below the thermocline (examination of target strengths around these shoals indicated that they were not juvenile walleye pollock). The offshore region had fewer fish shoals but extensive plankton patches rising up from the bottom near the end of the transect (near dusk), showing that many plankton are close to the bottom during daytime.

GAM results show the effect of plankton biomass index on walleye pollock biomass index in each bin, along with 95% confidence limits, obtained by bootstrap resampling of the data (Fig. 6). Regressions were significant for the front ($p = 0.001$) and offshore ($p = 0.0009$) regions, suggesting that age-0 walleye pollock biomass index increased with increasing plankton biomass index up to 0.01 and then decreased with higher plankton levels and subsequently increased at high plankton levels only in the offshore region. There were too few data in the nearshore region for a meaningful GAM regression.

Results for the distance-based proximity measure for each of the transect A regions are given in Fig. 7. There was significant clustering of plankton around the fish shoals in the nearshore and front regions (the empirical curve is above the upper 95% confidence limit), while in the offshore region, which contained large plankton patches, the distribution was random (the empirical curve is between the upper and lower 95% confidence limits), except at *h* between 0 and 100 m (Fig. 7*c*). Since this was a daytime transect, there tended to be separation of the plankton and fish, with fish being in the upper water column and plankton near the bottom (Fig. 4). Despite this separation, there is evidence that the fish remained closer to the plankton than would be indicated by a random horizontal distribution of the plankton patches, especially in the nearshore and front regions. Alternatively, from a fish shoal's spatial perspective, there were more plankton patches in the nearshore and front regions within 1 km of the fish shoals than there would have been if the zooplankton patches had been randomly distributed.

The GAM results are consistent with findings of the distance-based proximity. Both suggested a stronger association between fish shoals and plankton patches when plankton biomass was lower. The random distribution of plankton patches around fish shoals and the reduction in fish shoal biomass index at high plankton density, as was observed in the offshore region, both suggest that there was a threshold density of plankton above which there was no small-scale spatial association between fish and plankton. Considering the existence of large plankton patches in the offshore region (Fig. 4), the lack of small-scale proximity between walleye pollock and zooplankton is not surprising. Because these findings are based on only a single transect pass, interpretation of these results must be considered preliminary, and a more complete analysis of this survey data, with a compari-

[3] The distribution is complicated by an edge effect to correct for patches that might partially lie outside the region of interest. This is accomplished by limiting the generated patch locations such that their edges must lie within the study region.

Fig. 6. GAM results for 250-m bins for transect A, September 19, 1995, daytime. Smooths show the effect of plankton on walleye pollock biomass index in the (*a*) front and (*b*) offshore regions. The rug (tick marks) along the bottom of each graph shows the location of the data points. The 95% confidence limits are shown with broken lines.

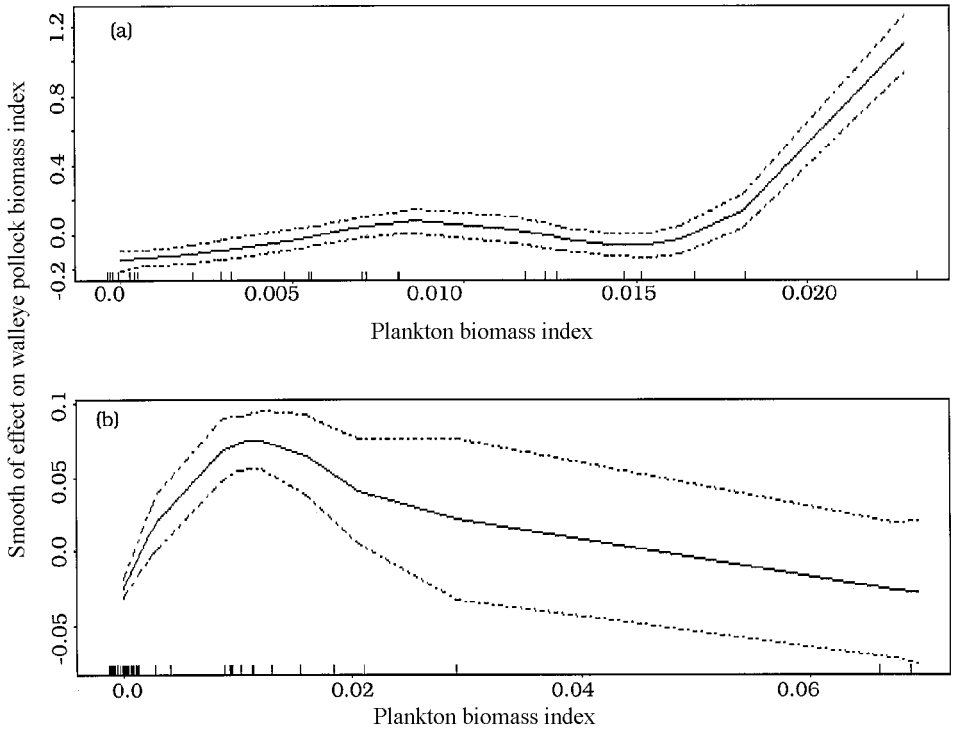

Fig. 7. Results of horizontal proximity measure for a daytime pass of transect A on September 19, 1995, in the (*a*) nearshore, (*b*) front, and (*c*) offshore regions. The nearshore and front regions show clustering of plankton patches around fish shoals, while in the offshore region the plankton patches appear to be randomly distributed around the fish shoals, except between 0 and 100 m distance (clustered). The empirical proximity measures are shown with solid lines and the 95% upper and lower confidence limits are shown with broken lines.

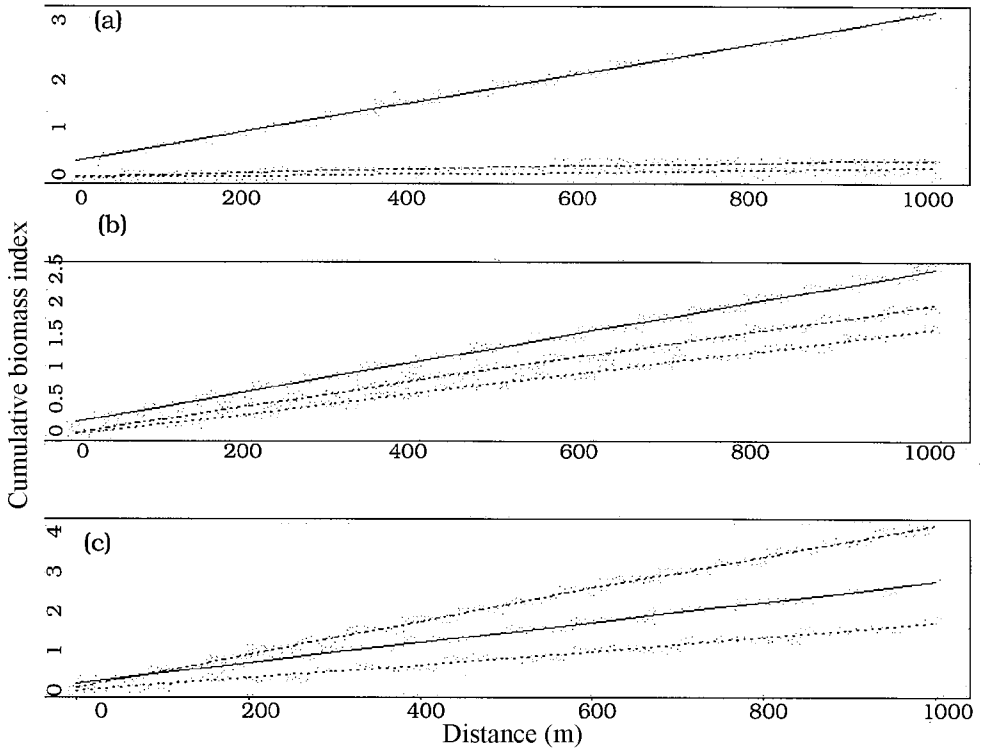

son between transects, day and night passes, and years, is needed.

Discussion

As our ability to effectively distinguish between acoustic measures of fish and plankton in marine ecosystems improves, we are confronted with new challenges in describing and testing their spatial relationship with a view to understanding marine feeding strategies and its repercussions for population dynamics and energetics. The amount of data and the computational demands of processing these data engender a need for visual display tools that can help scientists to examine their data in an explicit spatial context and can allow them to examine and critique the analysis tools used. The FishViewer point-and-click acoustic data viewer presented here is one such tool, hopefully a precursor of many such exploratory data analysis aids for acoustic and accompanying oceanographic and biological data.

We have found the development of algorithms to delineate plankton from juvenile fish patches in acoustic data to be a challenge. We have reported on our current algorithm in the hope that it will be tested and improved with application to other data sets, as has already occurred with the fish identification algorithm that we used (Reid and Simmonds 1993; Swartzman et al. 1994*a*). Our plankton delineation algorithm used data at two frequencies and depended on smaller organisms like plankton giving higher backscatter at higher frequencies, while juvenile fish have very small frequency dependence in their target strengths at these frequencies. A test of the algorithm could be made by comparing the depth distribution of acoustically determined plankton with the depth distribution of zooplankton sampled by accompanying net samples. A stronger test would involve doing the forward calculation on the net survey plankton (Greenlaw 1979; Stanton et al. 1993) to predict what the backscatter from the net-sampled organisms ought to be. We could then ascertain whether the predicted backscatter (in limited areas where net samples were available) agrees with the observed backscatter.

Establishing and interpreting spatial proximity between fish and plankton is complicated by the patchy nature of their spatial organization and temporal change in their distribution (daily, seasonal, and annual). Binning data represents one approach to examining such proximity but has the distinct disadvantage of defining proximity only by horizontal overlap and not distance or depth overlap. In cases where many of the patches are large, as they were in this survey, a distance-based proximity measure including the shape, orientation, and location is desirable. The distance-based proximity test combines a measure of distance between patches with a measure of patch size (biomass index). It extends the strictly biomass index based GAM measure of overlap over horizontal space to examine proximity within a wider area of influence. Furthermore, the distance-based measure takes the existing patches as a baseline measure and examines how proximity would change if the same patches were randomly arranged horizontally over the area of interest. The GAM interval-based measure achieves its confidence limits through bootstrap resampling (not random reorientation) of both the plankton patches and the fish shoals. A more significant GAM relationship derives from narrower confidence limits. Significance in the distance-based proximity measure is also dependent on the confidence limits because wide confidence limits are more likely to lead to the distribution being random.

The two measures define different aspects of proximity. The interval-based measure (GAM) indicated biomass index ranges for the covariate (plankton biomass index) over which the dependent variable (fish biomass index) increased and beyond which it decreased. This could suggest a density threshold above which feeding rate is maximum, thereby necessitating no spatial association. Alternatively, it could suggest depletion of plankton by higher fish biomass index concentrations. The distance-based measure suggested clustering of plankton patches around fish shoals in the nearshore and front regions. The degree of clustering was highest in the nearshore region (as indicated by the empirical curve being much higher than the upper 95% confidence limit), where plankton biomass index was lowest (Fig. 7). In the offshore region, with the highest plankton biomass index (Fig. 4), the plankton were randomly distributed about the fish shoals (the empirical curve is between the upper and lower 95% confidence limits), except at 0 distance (Fig. 7). This also suggests that at higher plankton densities, there was no spatial association between fish and plankton over a horizontal distance range from 100 m to 1 km.

We have chosen to examine the distance-based proximity of plankton patches to fish shoals. We could also examine the proximity of fish shoals to plankton patches — a prey spatial view of their predator. The two measures are not symmetric. We chose the former approach because we perceived the feeding age-0 walleye pollock as more likely to make a behavioral choice around association with their prey that involved horizontal swimming than would the plankton, who appear to use diel migration as a defense against predation.

Horizontal distance and vertical distance are clearly perceived differently by fish and plankton. Thus, we considered several alternative distance measures, although none of them addresses the nonlinearity of the vertical thermocline barrier. One option not considered is to treat above- and below-thermocline biota separately. However, this would neglect the diel migration of plankton. Thus, some of the plankton below the thermocline during the daytime, although they have no physical overlap with the above-thermocline fish, will at night move up near the thermocline and become accessible to these fish. So the daytime proximity measure, if spatial association is the desired criterion, might well ignore the vertical separation, as we did with the walleye pollock – plankton data by using the horizontal distance measure.

Differences in the magnitude of the distance-based proximity measure can be used to compare how much plankton biomass is available to fish shoals in different regions, at different times of the year, or in different years. Such comparisons are possible in a multiyear, multiple-transect study. For example, the low biomass index in the nearshore region (Fig. 7*a*) corroborates that there were fewer prey available for walleye pollock than in the front and offshore regions (Brodeur et al. 1997). As such, we would expect that walleye pollock were less abundant in the nearshore region, which they were.

The proximity tests (both the overlap and biomass indexes) may have general applicability in ecology, particu-

larly in areas where biota aggregate, such as burrowing animals, flocking birds, and herding animals. In fisheries, many juvenile pelagic fish, both marine and freshwater, shoal. For these aggregative groups, distance-based proximity measures may help uncover spatially explicit feeding phenomena not observable with interval-based measures of overlap. The two measures, taken together, can supplement each other to strengthen hypotheses and provide possible insight into spatial interactions between organisms. Working with a proximity index that combines distance, shape, and size of patches has considerable appeal in a situation where the patches cover a significant amount of the study region. Results from the current study, and the widespread nature of aggregation in marine ecosystems, warrant further proximity measure development, analysis, and testing.

Acknowledgments

This is contribution No. B-311 to the Fisheries–Oceanography Cooperative Investigation (FOCI). Funding for this project was provided by the National Oceanographic and Atmospheric Administration (NOAA) Coastal Ocean Program (COP) as part of the Southeast Bering Sea Carrying Capacity Project (SEBSCC). The authors wish to thank Phyllis Stabeno and Sigrid Salo for providing valuable interpretation of oceanographic data and Lorenzo Ciannelli for helpful comments on earlier drafts of this paper. Helpful and incisive reviews were provided by Pierre Petitgas and an anonymous reviewer. Finally, we greatly appreciate the thoughtful editorial and organizational suggestions by series editor Doran Mason.

References

Barange, M. 1994. Acoustic identification, classification and structure of biological patchiness on the edge of the Agulhas Bank and its relation to frontal features. S. Afr. J. Mar. Sci. **14**: 333–347.

Becker, R.A., Chambers, J.M., and Wilks, A.R. 1988. The new S Language. Wadsworth, Pacific Grove, Calif.

Brodeur, R.D., and Wilson, M.T. 1996. Mesoscale acoustic patterns of juvenile walleye pollock (*Theragra chalcogramma*) in the western Gulf of Alaska. Can. J. Fish. Aquat. Sci. **53**: 1951–1963.

Brodeur, R.D., Wilson, M.T., Napp, J.M., Stabeno, P.J., and Salo, S. 1997. Distribution of juvenile pollock relative to frontal structure near the Pribilof Islands, Bering Sea. *In* Proceedings of the International Symposium on the Role of Forage Fishes in Marine Ecosystems. Alaska Sea Grant Publ. AK-SG-97-01. pp. 573–589.

Brown, J.S., and Morgan, R.A. 1995. Effects of foraging behavior and spatial scale on diet selectivity — a test with fox squirrels. Oikos, **74**: 122–136.

Clay, C.S., and Medwin, H. 1977. Acoustical oceanography. John Wiley & Sons, Inc., New York.

Cressie, N.A.C. 1993. Statistics for spatial data. John Wiley & Sons, Inc., New York.

Diggle, P.J. 1983. Statistical analysis of spatial point patterns. Academic Press, London, U.K.

Foote, K.G., Knudsen, H.P., Vestnes, G., MacLennan, D.N., and Simmonds, E.J. 1987. Calibration of acoustic instruments for fish density estimation: a practical guide. Int. Counc. Explor. Sea Coop. Res. Rep. No. 144.

Greenlaw, C.F. 1979. Acoustical estimation of zooplankton populations. Limnol. Oceanogr. **24**: 226–242.

Haralick, R., and Shapiro, L. 1992. Image analysis. VI. Addison-Wesley, New York.

Hastie, T., and Tibshirani, R. 1990. Generalized additive models. Chapman and Hall, London, U.K.

Holliday, D.V., and Pieper, R.E. 1980. Volume scattering strengths and zooplankton distributions at acoustic frequencies between 0.5 and 3 MHz. J. Acoust. Soc. Am. **67**: 135–146.

Horne, J.K., and Schneider, D.C. 1994. Lack of spatial coherence of predators with prey: a bioenergetic explanation for Atlantic cod *Gadus morhua* feeding on capelin *Mallotus villosus*. J. Fish Biol. **45**(Suppl. A): 131–142.

Lascara, K. 1997. SCANFISH transect visualization tool. http://www.ccpo.odu.edu/~lascara/Ties/ties.html.

Mackas, D.L., Denman, K.L., and Abbott, M.K. 1985. Plankton patchiness: biology in the physical vernacular. Bull. Mar. Sci. **37**: 652–674.

Mackas, D.L., Kieser, R., Saunders, M., Yelland, D.R., Brown, R.M., and Moore, D.F. 1997. Aggregation of euphausiids and Pacific hake (*Merluccius productus*) along the outer continental shelf off Vancouver Island. Can. J. Fish. Aquat. Sci. **54**: 2080–2096.

Mann, K.H., and Lazier, J.R.N. 1991. Dynamics of marine ecosystems. Blackwell Scientific Publications, Cambridge, Mass.

Maravelias, C.D., and Reid, D.G. 1997. Identifying the effects of oceanographic features and zooplankton on prespawning herring abundance using generalized additive models. Mar. Ecol. Prog. Ser. **147**: 1–9.

Mullin, M.M. 1993. Webs and scales: physical and ecological processes in marine fish recruitment. Univ. Wash. Sea Grant Publ. WSG-IS-93-01.

Nero, R.W., and Magnuson, J.J. 1989. Characterization of patches along transects using high-resolution 70-kHz integrated acoustic data. Can. J. Fish. Aquat. Sci. **46**: 2055–2064.

Precision Visuals. 1992. Command language users guide. Precision Visuals, Boulder, Co.

Reid, D.G., and Simmonds, E.J. 1993. Image analysis techniques for the study of fish school structure from acoustic survey data. Can. J. Fish. Aquat. Sci. **50**: 886–893.

Rose, G.A., and Leggett, W.C. 1990. The importance of scale to predator–prey spatial correlations: an example of Atlantic fishes. Ecology, **71**: 33–43.

Stabeno, P.J., Schumacher, J.D., Salo, S.A., Hunt, G.L., and Flint, M. 1999. The physical environment around the Pribilof Islands. *In* The Bering Sea: physical, chemical and biological dynamics. *Edited by* T.R. Loughlin and K. Ohtani. Alaska Sea Grant Press, Anchorage, Alaska. In press.

Stanton, T.K., Chu, D., Wiebe, P.H., and Clay, C.S. 1993. Average echoes from randomly oriented random-length finite cylinders: zooplankton models. J. Acoust. Soc. Am. **94**: 3463–3472.

Swartzman, G.L. 1997. Analysis of the summer distribution of fish schools in the Pacific Eastern Boundary Current. ICES J. Mar. Sci. **54**: 105–116.

Swartzman, G.L., Stuetzle, W., Kulman, K., and Wen, N. 1994*a*. Modeling the distribution of fish schools in the Bering Sea: morphological school identification. Nat. Resour. Model. **8**: 177–194.

Swartzman, G., Stuetzle, W., Kulman, K., and Powojowski, M. 1994*b*. Relating the distribution of pollock schools in the Bering Sea to environmental factors. ICES J. Mar. Sci. **51**: 481–484.

Traynor, J.J. 1996. Target strength measurements of walleye pollock (*Theragra chalcogramma*) and Pacific whiting (*Merluccius productus*). ICES J. Mar. Sci. **53**: 253–258.

Wiebe, P.H, Greene, C.H., Stanton, T.K., and Burczynski, J. 1990. Sound scattering by live zooplankton and micronekton: empirical studies with a dual-beam acoustical system. J. Acoust. Soc. Am. **88**: 2346–2360.